

## Active Force Control of a 5-Link Biped Robot

L.C. Kwek<sup>1</sup> C.K. Loo<sup>2</sup> E.K. Wong<sup>3</sup> M.V.C Rao<sup>4</sup> M. Mailah<sup>5</sup>

<sup>1,2,3,4</sup> Faculty of Engineering and Technology

Multimedia University, Jalan Ayer Keroh Lama, 75450 Melaka, Malaysia.

<sup>1</sup>Tel: +606-2523276, Fax: +606-2316552, E-mail: lckwek@mmu.edu.my

<sup>2</sup>Tel: +606-2523276, Fax: +606-2316552, E-mail: ckloo@mmu.edu.my

<sup>3</sup>Tel: +606-2523251, Fax: +606-2316552, E-mail: ekwong@mmu.edu.my

<sup>4</sup>Tel: +606-2523726, Fax: +606-2316552, E-mail: machavaram.venkata@mmu.edu.my

<sup>5</sup> Faculty of Mechanical Engineering

University Technology of Malaysia, 81310 Skudai, Johor, Malaysia.

<sup>5</sup>Tel: +607-5504554, ext.4735, Fax: +607-2316552, E-mail: musa@fkm.utm.my

### Abstract

The performance of the biped system under the application of Active Force Control (AFC) is evaluated by making the biped walk on a horizontal plane surface, in which the locomotion is constrained within the sagittal plane. The dynamic equations for a biped are nonlinear and highly coupled, and hence the biped does not perform well with the pure PD control. The effectiveness of the proposed method (Active Force Control with Crude Approximation-AFC-CA) is investigated and it is found that the system is robust and stable even under the influence of disturbances.

### Keywords:

Biped, Proportional-Derivative, Active Force Control, Crude Approximation.

### 1.0 Introduction

A biped robot possesses the potential of human-like mobility, especially moving on rough terrain, steep stairs and obstructed environments. Thus, they can operate in the irregular and unknown environments, and even replace humans in hazardous environment such as nuclear power plants, polluted areas and ocean floors.

Control approaches developed for bipeds are generally based on simplified robot dynamics. Some researchers have studied the use of neural networks as an on-line method. Benbrahim and Franklin have used reinforcement learning algorithms for a biped to achieve dynamic walking. Miller designed a neural network learning system for a biped that was capable of learning the balance from side-to side and front-to-back motion [2]. There were also some further contributions as in [3]. Spyros et al investigated pure computed torque control and robust sliding-mode control applied to a 5-link biped [1]. Lum et al extended their work by proposing a robust variable structure control to the similar biped model. [4].

Biped walking robots are typical systems affected by uncertainties and disturbances. The leg kinematics and dynamics are highly nonlinear and known with low accuracy, gait length depends on types of surfaces. Active Force Control (AFC) has been proposed as an alternative to handle disturbance compensation [5] for robotic systems since 1981. The approach of AFC is to measure and estimate control parameters, thus reducing the computational burden. In this paper, a conventional crude approximation is used together with the AFC strategy to control a biped robot.

### 2.0 The 5-Link Biped Model

In this case, Lagrangian equation has been used to obtain the mathematical model of the biped system. Initially, the kinematics model of the biped will be presented [1].

#### 2.1 Kinematics Model

Figure 1 illustrates the planar biped model used in this study.

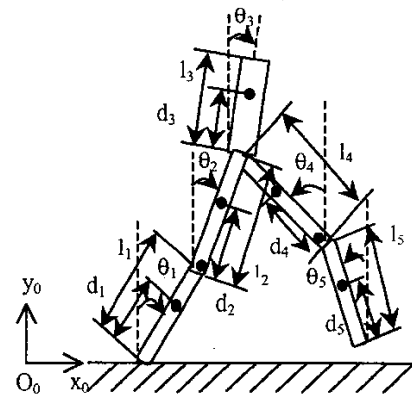


Figure 1 - Biped in single-leg-support phase

The biped consists of five links, namely the torso (link3) and two links in each leg (the upper legs, that are links 2 and 4, and the lower legs, that are links 1 and 5). These links are connected via four rotating joints (two hip joints and two knee joints), which are considered to be friction free and each of the joints is driven by an independent DC motor. It is assumed that the locomotion of the biped is constrained within the sagittal plane. The robot does not possess ankle joints and feet, thus, the base areas of the legs (links 1 and 5) are assumed to be large enough to maintain its balance at vertical positions.

Due to the space constraint, the physical parameters shown in Figure 1 are eliminated from here, readers can find this information in [4].

## 2.2 Dynamic Model

The motion of biped robots is achieved via the phased movements of the legs, that is by gait which the legs must alternate between support (on the ground) and transfer phases (in the air) in order to propel the robots forward. The motion of the biped is divided into three distinct phases - single-leg-support, double-leg-support, and biped in the air. In general, the dynamic performance of the biped robot can be written as [1],

$$D(\theta) \cdot \ddot{\theta} + h(\theta, \dot{\theta}) + G(\theta) = T_o \quad (1)$$

where  $D(\theta)$  is a 5x5 symmetric, positive-definite inertia matrix,  $h(\theta, \dot{\theta})$  is a 5x1 column vector consisting of coriolis and centripetal torques,  $G(\theta)$  is a 5x1 gravity vector, and  $T_o$  is the generalized torque that corresponds to  $\theta_i$ .

## 3.0 The Control of the Biped

A controller plays a pertinent role to initiate, terminate, and coordinate the motion and sequences of a robot. Basically, the aim of employing robotic control scheme is twofold. To provide the coordinate motion control of the robot which particularly deals with the trajectory tracking performance and reject noise and disturbance in the system without degrading the performance.

### 3.1 The Proportional-Derivative (PD) Control

Proportional-Derivative (PD) controller is one of the most popular conventional controllers being used, as it is computationally simple and with reasonably robust.

Let  $a$  being the auxiliary control signal of the PD controller, we have,

$$a = \ddot{\theta}_{bar_i} + K_D (\dot{\theta}_{bar_i} - \dot{\theta}_i) + K_P (\theta_{bar_i} - \theta_i) \quad (2)$$

where  $\theta_{bar_i}$ ,  $\dot{\theta}_{bar_i}$ , and  $\ddot{\theta}_{bar_i}$  are the desired reference joint trajectory, desired reference velocity, and desired reference

acceleration for link  $i$  respectively, while  $\theta_i$  and  $\dot{\theta}_i$  are their actual counterparts

To obtain a critically damped closed-loop performance, the PD gains must be chosen in such a way that,

$$K_D = 2\lambda \quad (3)$$

$$\text{And, } K_P = \lambda^2 \quad (4)$$

where  $\lambda$  is the desired bandwidth [4]. However, the PD control though simple and stable could only provide satisfactory performance at a low speed operation.

### 3.2 The Active Force Control (AFC) Scheme

The idea of AFC is first coined by Hewit and Burdess [5]. The goal of this control scheme is to ensure that a system remains stable and robust even in the presence of disturbances. AFC involves direct measurement or estimation of a number of identified parameters to effect its compensation action. Hence, a large portion of mathematical and computational burden can be eliminated. From the Newton's second law of motion, for a rotating mass, i.e.

$$\Sigma T = I\ddot{\theta} \quad (5)$$

where  $T$  is the sum of all torques acting on the body,  $I$  is the moment of inertia, and  $\ddot{\theta}$  is the angular acceleration.

For a robot system, the motion equation becomes

$$T + Q = I(\theta)\ddot{\theta} \quad (6)$$

where  $T$  is the applied torque,  $Q$  is the disturbance torques,  $I(\theta)$  is the moment inertia,  $\theta$  and  $\ddot{\theta}$  are the joint angle and angular acceleration of the robot respectively.

The disturbance torques or "noises" in a robotic manipulator are made up of the Coriolis, centrifugal and frictional forces. The estimated value of the disturbance torque,  $Q'$  can be formulated as

$$Q' = I'(\theta)\ddot{\theta}' - T' \quad (7)$$

where the superscript ' denotes a measured or computed value.  $Q'$  can be used to decouple effect of the actual disturbance torque  $Q$ , hence the system will be stable even under variable external force. In this context, the applied torque  $T'$  can be measured by using a force (or current) sensor, and the angular acceleration of the robot,  $\ddot{\theta}'$  can be measured by using an accelerometer. On the other hand, the mass moment of inertia,  $I'$  can be obtained by conventional methods or intelligent approaches.

Considering the schematic in Figure 2, there are two types of controller applied to a biped, viz., the Proportional-Derivative (PD) control and Active Force Control (AFC).

The PD controller gives the required control signal,  $\ddot{\theta}_{ref}$ , as shown in Figure 2.

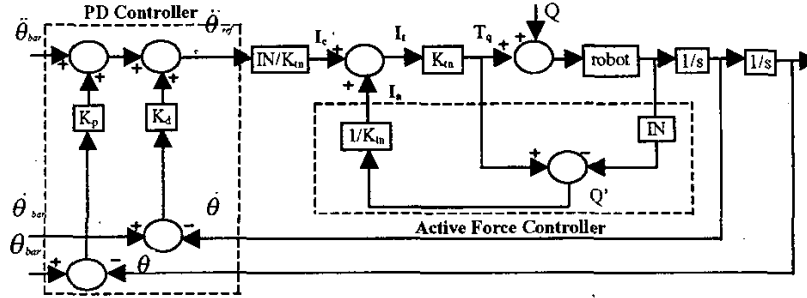


Figure 2 - The block diagram of the PD and AFC strategies applied to a biped

On the other hand, the AFC loop compensates the actual disturbance torque,  $Q$ . An estimated value, which is obtained from the error between the ideal and actual force vectors, is required to carry out the subsequent movement. The error provides an adjustment signal to the actuation system. From Figure 2, the estimated disturbance  $Q'$  can be described as,

$$Q' = IN\ddot{\theta} - T_q \quad (8)$$

$$T_q = I_t K_m \quad (9)$$

where  $IN$  is the estimated inertia matrix,  $\ddot{\theta}$  is the acceleration signal,  $T_q$  is the applied control torques,  $K_m$  is the motor constant, and  $I_t$  is the armature current for the torque motor.  $I_t$  is the sum of  $I_c$  and  $I_a$  where  $I_c$  is the current command vector and  $I_a$  is the compensating current vector representing the disturbance.

However, efficiency of the AFC strategy relies heavily on the inertia matrix estimator. In this paper, a crude approximation method has been used to estimate the inertia matrix.

### 3.2.1 Active Force Control and Crude Approximation (AFC-CA)

To obtain the estimated inertia matrix  $IN$ , an approximation factor namely the "coefficient of the estimated inertia matrix",  $K_{in}$  is to be multiplied with the diagonal terms of the inertia matrix,  $H$  from the dynamic model,

$$[IN] = K_{in} * [H]_{diag} \quad (10)$$

The procedure of obtaining the optimum  $K_{in}$  is given below:

1. The diagonal terms of the inertia matrix from the model,  $H$  was first derived mathematically.
2. A coefficient,  $K_{in}$  was embedded into the simulation program. This factor will be multiplied with  $H$  and subsequently fed into the AFC loop.
3. An initial value of  $K_{in} = 1.0$  was assumed, implying that the full  $H$  model was first considered.

4. The simulation program was executed. The average tracking error,  $ATE$  was observed and recorded.
5. Steps 3 and 4 were repeated by using different value of  $K_{in}$ . In this study,  $K_{in} = 0.2, 0.4, \dots, 4.0$  with varying step sizes are used.
6. Finally, a graph of  $ATE$  vs.  $K_{in}$  representing the performance was plotted to get optimum  $K_{in}$ .

## 4.0 Simulation

In this study, the simulation work is performed by using the <sup>2</sup>MATLAB and SIMULINK software packages.

The robot parameters are obtained from the work in [1]. For the PD controller,  $\lambda = 30/s$  has been used (by considering the possible saturation of the motors). Thus, the controller gains are  $K_p = 900/s^2$  and  $K_d = 60/s$ . The motor torque constant  $K_m = 0.263Nm/A$  is obtained from the actual data sheet for the DC torque motor.

In order to examine the stability of the biped system, a standard test input signal - the step input has been used as the reference input (joint angles) for the biped. Reference joint angles,  $\theta_{bar1}$  have been set such a way that  $\theta_{bar1} = 0.385rad$ ,  $\theta_{bar2} = 0.370rad$ ,  $\theta_{bar3} = 0.100rad$ ,  $\theta_{bar4} = 0.260rad$ ,  $\theta_{bar5} = 0.050rad$ .

Here, the pure PD control scheme and the proposed AFC-CA control method have been used in order to keep the joint angles of the biped close to the reference function given. The simulation period is set to 2.00s. An external disturbance force, pulsating torques with amplitude of 50N, period of 0.50s and duty cycle of 10% of period is enforced on the biped.

## 5.0 Results and Discussions

### 5.1 The pure PD control

The graphical results gained from the simulation by using pure PD controller are shown in Figure 3a - 3b. Figure 3a

<sup>1</sup>  $ATE$  is defined as the average tracking error generated by all of the 5 axes of the biped during a specified simulation period.

<sup>2</sup> MATLAB and SIMULINK are registered trademarks of The Math Works Inc.

illustrates the actual joint angles of the biped. It is noticed that the joint angles become distorted when the pulsating torques are activated.

The track error signals generated are depicted in Figure 3b. The errors obtained are considerably large, i.e., for axis-1, the track error = 0.048rad at the end of the simulation. This contributes to 12.47% from the desired reference value.

### 5.2 The AFC-CA control scheme

The optimum value of  $K_{in} = 4.2$  has been determined from the performance curve. The simulation program has been repeated by using this  $K_{in}$  value.

Figure 4 a - 4b illustrates the graphical results gained from the simulation by using the AFC-CA control scheme. Figure 4a illustrates the actual joint angles of the biped. It is noticed that the biped using AFC-CA strategy takes less time to keep its joint angle to be close to the reference input, i.e., for axis-1, the biped takes 0.31s to remain within 0.16% of its desired reference value. Besides, there are no overshoot problems for all of the axes, except axis-5.

The track error generated by the biped is shown in Figure 4b. It is noticed that the error margin is significantly smaller than that of the pure PD control model. The AFC-CA scheme manages to keep the error margin to be below 0.0203rad (for all of the five axes) after 0.54s.

The overall performance of the pure PD controller and the proposed AFC-CA can be compared from the viewpoint of *ATE* of the biped for all of the 5 axes for 2s. From the results gathered from the simulation studies, the *ATE* of the biped by using pure PD control equals to 0.1604rad whereas the *ATE* of AFC-CA equals to 0.0408rad.

The performance of the biped has been improved dramatically by using the proposed control scheme. It is also noticed that the biped by using AFC-CA control strategy takes less time to recover to its stable state.

### 6.0 Conclusions

The simulation results have shown the performance of the biped with AFC-CA is superior to that of the PD control. The learning strategy enables the trajectory track error to remain in an acceptable margin in which the actual joint trajectory resembles the desired one. The biped learns in a reasonably fast rate in which the resultant tracking error generated after 0.54s is below 0.0203rad for all axes. Furthermore, the *ATE* value generated by the biped by using the proposed control scheme is merely 25% of that from the conventional PD control.

### References

- [1] S. Tzafestas, M. Raibert, C. Tzafestas. 1986. Robust sliding-mode control applied to a 5-link biped robot. *Journal of Intelligent and Robotics Systems* 15:67-133.
- [2] Miller W.T. 1994. Real-Time Neural Network Control of a Biped Walking Robot. *IEEE Control Systems* 14(1):41-48
- [3] Jiangjue Hu, Pratt J., and Pratt G. 1998. Adaptive Dynamic Control of a Biped Walking Robot with Radial Basis Function Neural Networks. In Proceedings of IEEE/RSJ International Conference on Intelligent Robots and Systems, 400-405.
- [4] H.K. Lum, M. Zribi, Y.C. Soh. 1999. Planning and control of a biped robot. *International Journal of Engineering Science* 37:1319-1349.
- [5] J.R. Hewit, J.S. Burdess. 1981. Fast Dynamic Decoupled Control for Robotics Using Active Force Control, *Mechanism and Machine Theory* 16(5):535-542.
- [6] M. Mailah. 1998. Intelligent Active Force Control Of A Rigid Robot Arm Using Neural Network And Iterative Learning Algorithms. Ph.D. diss., University of Dundee, Dundee.

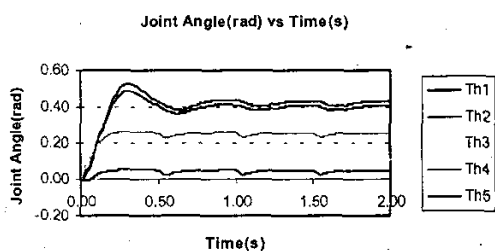


Figure 3a - Actual joint angle,  $\theta_i$  from PD

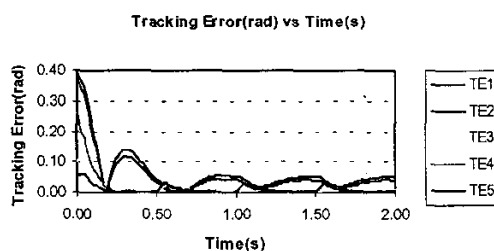


Figure 3b - Tracking error,  $TE_i$  from PD

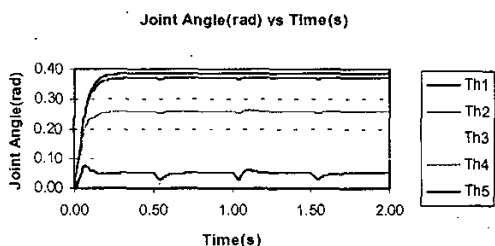


Figure 4a - Actual joint angle,  $\theta_i$  from AFC-CA

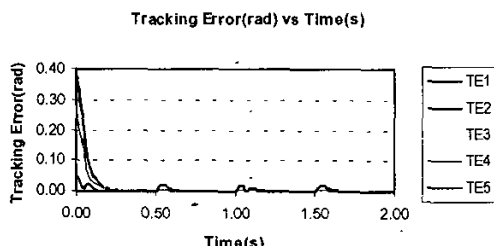


Figure 4b - Tracking error,  $TE_i$  from AFC-CA